Hindawi
Wireless Communications and Mobile Computing
Volume 2022, Article ID 4320297, 10 pages
https://doi.org/10.1155/2022/4320297

*Research Article*

# Migration Path Tracking Algorithm of Egret Birds Based on Intelligent Remote Sensing Monitoring

**Liping Li**

*School of Biological Engineering, Hunan Polytechnic of Environment and Biology, Hengyang, 421000 Hunan, China*

Correspondence should be addressed to Liping Li; llp@hnebp.edu.cn

Received 9 June 2022; Revised 21 July 2022; Accepted 12 August 2022; Published 30 August 2022

Academic Editor: Chia-Huei Wu



There are billions of migratory birds migrating between breeding grounds and wintering grounds in the world every year. Egret is no exception. During the migration period, they need to travel for a long time and long distances. At present, the protection strategies of egrets and the dynamic mechanism of migration routes are concerned by experts in related fields. Researchers generally explore the above problems by tracking the migration paths of egrets. Most of the existing path tracking algorithms use some classical tracking algorithms, but the tracking accuracy of the classical algorithms is low. Therefore, this paper has applied the intelligent remote sensing monitoring technology to the improvement of the path tracking algorithm, used artificial intelligence technology to remove the redundant information of the image, and combined the Kalman filter with the single-target long-term algorithm to improve the tracking algorithm. 100 samples were simulated, and the experimental results showed that the tracking accuracy of the egret bird migration path tracking algorithm based on intelligent remote sensing monitoring was improved by 8.37% compared with the algorithm before improvement, which has better utilization value.

## 1. Introduction

Birds of the egrets are divided into four species: large, medium, small, and yellow-billed egrets. Because of its white feathers, good beauty, and high value, the Egret genus has been indiscriminately killed by humans and is currently defined as an endangered species. Relevant experts have made certain efforts in the exploration and formulation of protection strategies for egrets and have developed a method for tracking the migration paths of egrets. However, the tracking accuracy of the algorithm used is low, which hinders the tracking work to a certain extent. Therefore, this paper designs a path tracking algorithm based on intelligent remote sensing monitoring, which can quickly measure the target center position of the current picture frame, and it adjusts the position to match the size of the monitoring window to the target size, minimizes the search area to reduce the number of monitoring windows, improves the monitoring accuracy of the algorithm, and also enhances the real-time performance of the algorithm. The improved algorithm can better track the migration paths of egrets, thus laying a foundation for the protection of egrets and related research.

Nowadays, there are many scholars' related research on path tracking algorithm: Dong et al. proposed a depth selection algorithm to identify characteristic probes from hundreds of thousands of complete probes and explored and analyzed the shortest path tracking method [1]. Yao et al. carried out wireless positioning and path tracking on the greenhouse mobile platform for a better performance of greenhouse research [2]. Zendehdel and Gholami designed a supervised two-level controller for autonomous underwater vehicle path tracking [3]. Pannekoucke et al. have addressed the model error from the theoretical perspective provided by the Kalman filter method and revisited the classical method of kinetically correcting equations [4]. Xia et al. have adopted methods based on integrated Kalman filters and stochastic equations of groundwater flow to explore three-dimensional stochastic heterogeneous fields of electrical conductivity and set up three types of observation devices for analysis of various configurations based on observation wells related synthesis test case. In addition, according to the standard deviation of the natural logarithm $Y$ of the conductivity, the use of the expansion factor imposed on the observation error covariance matrix is completed, and it is solved by the effective transient numerical scheme proposed in the study [5]. Dong et al. used the single-target long-time algorithm to track, learn, and monitor the moving vehicle for a long time from the video stream. The problem was found that caused the tracking failure in the algorithm, and an improved tracking algorithm was proposed [6]. The overspeed of some vehicles becomes an obstacle of tracking. Panda and Barczyk introduce the fast retinal keypoint feature in the tracker to mitigate instability caused by illumination changes or scale changes, obtain reliable bounding boxes, and improve tracking accuracy [7]. Quesada-Barriuso et al. proposed a graphics card algorithm for superpixel segmentation using a computationally unified device architecture. The algorithm extracts all spectral information available in the hyperspectral image through vector gradients and uses a block implementation with high connectivity to select cells to compute transform values [8]. Chen et al. have proposed a recognition method based on superpixel segmentation to solve the problem that the target segmentation is broken and difficult to be identified and monitored due to the complex background and shadow areas in satellite images. The objective quantity is first predetermined using the histogram of guided gradients, and then, the superpixel segmentation algorithm is finally improved by clustering pixels with the same features [9].

In addition, many scholars have conducted in-depth research on remote sensing monitoring technology: Ding et al. compared different state-of-the-art deep convolutional neural network models on two publicly available remote sensing datasets, namely, the aircraft dataset and the automobile dataset, which can provide guidance for relevant researchers [10]. Guo and Wang conducted an ecosystem risk assessment for a certain area based on multiscale, multitemporal remote sensing monitoring technology and land use data. In addition, a transfer trajectory analysis was carried out using the dynamic change information survey method to focus on land use change [11].

At present, scholars have made some achievements in the research of path tracking algorithm and intelligent remote sensing monitoring technology, but there are still many problems including inaccurate tracking and outdated skills for remote detection. In this paper, the intelligent remote sensing monitoring technology is applied to the improvement of the recommendation algorithm, focusing on solving the existing problems, which can better track the migration path of egret birds and promote the protection and related research of Egret birds.

## 2. Egrets' Migration Path Tracking Algorithm

In order to obtain the migration information of migratory birds in the early days, bird researchers waited for migratory birds in some specific places to observe their migration phenomenon, which was inefficient and difficult to observe and record the individual birds [12]. Later, some scholars caught birds through purse seine and other methods in places where birds are concentrated, such as breeding grounds, wintering grounds, or stopping places on the way to migrate. They put the rings with addresses or address numbers on the calves or tarsus of birds, then released them in situ, and then captured or observed them again in other places, so as to study the migration patterns of birds. This method was recognized by the ornithological community, named the ringing method, and was extended to the ornithological community for use [13]. Later, with the advancement of technology, some new methods were applied to bird migration research, and the means of bird research became more and more diversified, refined, and scientific, including but not limited to radio tracking and satellite track [14].

The difficulty in designing the algorithm for tracking the migration path of egret is that the vast majority of egrets fly at an altitude of less than 100 meters when migrating, which puts forward high requirements for the accuracy of remote sensing monitoring [15]. That is, the acquisition of images at a lower altitudes requires the support of power algorithm by remote detection. In addition, the migration strategies of egrets are related to individual personalities, so there are differences between migration strategies, which requires high real-time and flexibility of the path tracking algorithm. Figure 1 shows the migration path of an egret.

Figure 1 shows a typical, more extreme example. This egret only took about 77 hours to migrate from near 8 degrees south latitude to near 38 degrees north latitude, with a straight-line distance of about 3,000 kilometers. The maximum speed on the way reached 95 kilometers per hour, and the minimum height was 4 meters [16]. These data reflect that the required research path tracking algorithm must be highly accurate and real-time; otherwise, the purpose of tracking such egrets cannot be achieved.

(1) Architecture of path tracking algorithm

The migratory path tracking algorithm of egrets based on intelligent remote sensing monitoring studied in this paper is mainly composed of two modules: a tracking preprocessing module and a tracking implementation module. In the preprocessing module, the intelligent remote sensing monitoring technology acquires image sequence frames and performs three steps of image matching, geometric correction, and radiometric correction. To be specific, image matching prepares for the preprocessing work, geometric correction prepares for the monitoring window prefab, and radiometric correction can make the acquired images free from significant radiation interference. Then, the superpixel segmentation technology is used to segment the image into superpixel blocks with specific meanings to remove unnecessary image information and reduce the complexity of algorithm processing. In the tracking implementation module, the Kalman filter is combined with the single-target long-time algorithm. The Kalman filter is used as the predictor to determine the center position of the target, and the size of the monitoring window is automatically adjusted according to the situation to ensure the tracking accuracy.

The architecture of the path tracking algorithm is shown in Figure 2.

As shown in Figure 2, this paper has integrated the above tracking preprocessing module and tracking module to create a complete set of tracking algorithms for the target,

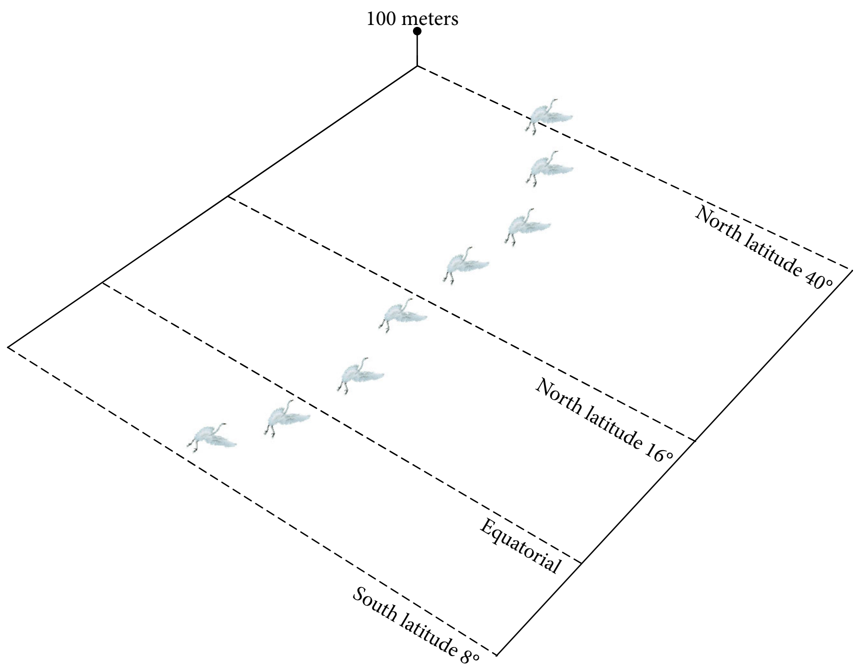


Figure 1: Migration path of an egret.

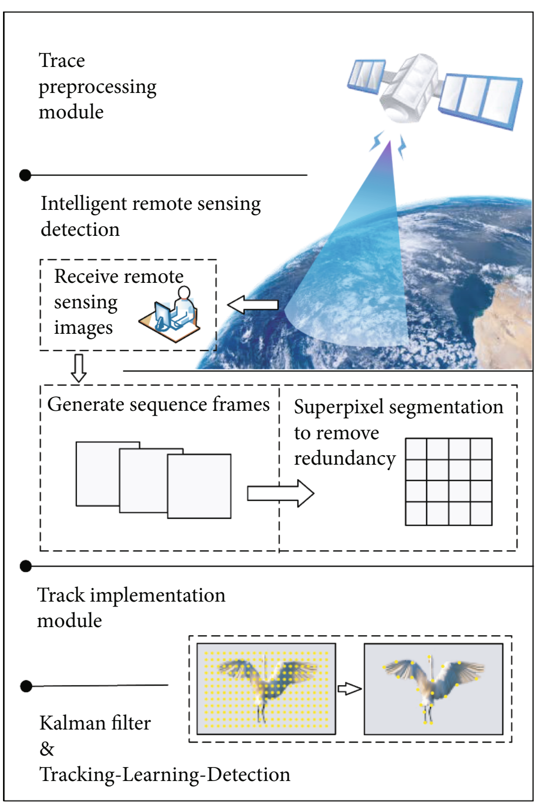


Figure 2: Path tracking algorithm architecture.

which can automatically find and track the target from the image sequence. The performance of the algorithm is thoroughly tested in this paper, and the experimental results show that the algorithm developed in this paper can consistently track the target in images with large background changes and images with specific characters and effectively adapt to the appearance of the target in flight various location information changes. The algorithm has high precision and strong real-time performance.

(2) Intelligent remote sensing monitoring to obtain image sequence frames

Remote sensing monitoring technology and visual imaging technology have made great progress with the continuous improvement of related theories and have been applied to survey of atmosphere, water quality, marine oil pollution, thermal environment, and ecological environment in society [17]. At present, remote sensing technology has been applied in many fields of society, including survey of atmosphere, water quality, marine oil pollution, thermal environment, and ecological environment in society. Remote sensing technology can be divided into three types: hyperspectral remote sensing, visible light remote sensing, and microwave remote sensing according to the different spectrum bands of electromagnetic waves used [18]. The traditional change monitoring method is visual interpretation, that is, the interpreter observes with the naked eye, and with the help of some auxiliary materials, the interpreter makes logical reasoning and then conducts a systematic and comprehensive analysis of the image [19]. Visual interpretation has many disadvantages, such as low degree of automation, long time consumption, and the need for a lot of human and financial support. In addition, there are some subjectivity limitations to this approach. For example, it is impossible to perform automatic learning iteration based on the results of previous monitoring, and it needs to be updated manually. The traditional methods of monitoring changes have been unable to meet the needs of society, so this paper has adopted a variety of methods to analyze remote sensing images, in order to quickly and efficiently monitor the changes in the target area.

The structure of intelligent remote sensing monitoring technology is shown in Figure 3.

As shown in Figure 3, the spatial information acquisition of egrets is mainly completed by the remote sensing platform and the data receiving and processing platform. The remote sensing platform is composed of spaceborne satellite sensing and UAV sensing. The data receiving and processing platform is composed of intelligent remote sensing technology center, data processing center, tracking and data receiving station, and command control station.

Intelligent remote sensing monitoring is a general term for a series of intelligent acquisition technologies for remote sensing image information [20]. These technologies rely on specific imaging tools to process remote sensing imaging information through a computer information detection system to display the shape and location of the target object. It consists of four parts: image editing, transformation, enhancement, and definition. Image editing refers to the targeted extraction of target-related information from remote sensing images and other remote sensing information. Image transformation transforms the original image into an image that can be easily calculated by the algorithm [21]. The focus of image enhancement is geometric alignment, which is to actively integrate remote images into 3D maps to provide enhanced information services for training. Image definition is the basis of intelligent remote sensing monitoring, including visual and computer description. It studies the remote sensing information through certain methods or models, determines the properties and characteristics of the target object, or deeply understands the internal relationship between the target object's attributes and the environment, so as to apply in specific fields or assist users in decision-making.

(3) Removal of image redundancy with artificial intelligence

Artificial intelligence technology is introduced here to solve the problem of tracking targets in remote sensing monitoring. There is a branch technology under the artificial intelligence algorithm: superpixel segmentation combined with graph segmentation based on graph theory. Superpixel segmentation based on graph theory is an artificial intelligence algorithm combined with graph segmentation. Its main generation principle is to use graphs with weights to map input images. When creating a computational flow for an undirected graph, each pixel embedded in the image corresponds to a node in the graph, and the dimension of each node connection is obtained by computing the difference between the functions of each pixel. Next, the algorithm uses some kind of splitting method on the undirected graph constructed above to achieve superpixel segmentation of embedded images. The method is shown in Figure 4.

As shown in Figure 4, when segmenting the input image, the minimum spanning tree algorithm [22] is needed. This algorithm is specially designed for image research and can process images in various ways. A minimum spanning tree in a weighted undirected graph corresponds to a region in the image, i.e., a superpixel unit [23]. The algorithm's intraregional interval, interregional differences, and merging rules are as follows:

(1) *Minimum Spacing within the Region*. Given a region C, the weight of each edge in it represents the difference between the two pixel endpoints of the edge, that is, the minimum interval in the region is the maximum weight value on the minimum spanning tree corresponding to the region, and the minimum interval in the region $\mathrm{Int}(C)$ is as follows:

$$\mathrm{Int}(C) = \max_{C \in \mathrm{MST}(C,E)} w\left(e_{ij}\right). \tag{1}$$

(2) *Differences between Regions*. During the modeling process, since each connected node in an undirected graph has a weight of its undirected edge, the weight can be expressed as the dissimilarity of the two connected pixel nodes. On the basis of obtaining the difference between nodes, the difference between any two different regions is expressed as the weight of the smallest edge connecting the vertices between these two regions:

$$\mathrm{diff}(\mathrm{C}_1, \mathrm{C}_2) = \min_{\mathrm{v_i} \in \mathrm{C}_1, \mathrm{v_j} \in \mathrm{C}_2, \left(\mathrm{v_i}, \mathrm{v_j}\right) \in E} \mathrm{w}\left(\left(\mathrm{v_i}, \mathrm{v_j}\right)\right). \tag{2}$$

(3) *Regional Merging Rules*. When merging regions, the superpixel generation algorithm based on graph theory does not use a global fixed threshold but uses the differences between regions and the interval within regions to adaptively determine whether two regions can be merged into one region. The merge criterion is shown in Equation (3).

$$\mathrm{D}(\mathrm{C}_1, \mathrm{C}_2) = \begin{cases} \text{true, if, } \mathrm{diff}(C_1, C_2) > \mathrm{MInt}(C_1, C_2), \\ \text{false, otherwise.} \end{cases} \tag{3}$$

$\mathrm{MInt}(C_1, C_2)$ represents the minimum division internal difference, and its calculation formula is as follows:

$$\mathrm{MInt}(\mathrm{C}_1, \mathrm{C}_2) = \min\left(\mathrm{Int}(\mathrm{C}_1) + \tau(\mathrm{C}_1), \mathrm{Int}(\mathrm{C}_2) + \tau(\mathrm{C}_2)\right). \tag{4}$$

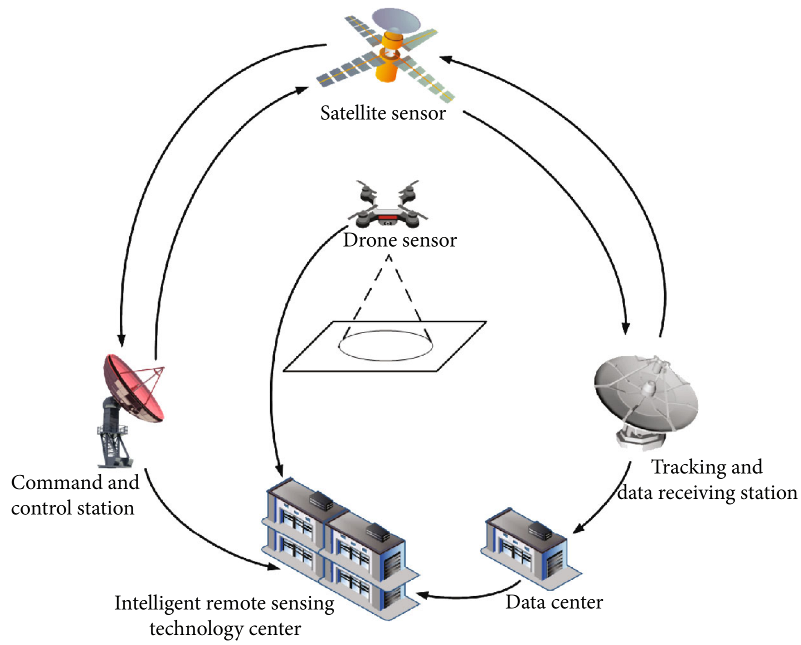


Figure 3: Intelligent remote sensing monitoring technology structure.

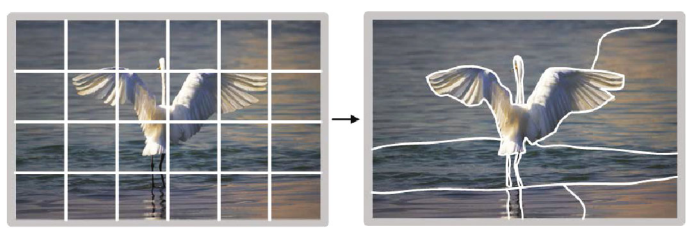

Figure 4: Superpixel segmentation.

The energy function is defined as follows:

$$E(S) = H(S) + \gamma G(S). \tag{5}$$

(4) Kalman filter combined with single-target long-time algorithm to improve path tracking algorithm

In this paper, the Kalman filter is combined with the single-target long-term algorithm. It is used to predict the position of the target in the current frame, and then, the monitoring area of the monitor in each frame is reduced to a certain range near the target position. The method can effectively narrow the monitoring range of the monitor and reduce the monitoring time.

(1) Establishment of Kalman filter model

The establishment of the Kalman filter model includes two main processes, namely, the prediction process and the verification process. The prediction process needs to use the iterative equation to establish the state variable value of the current time and create an estimated value for the next time state for prediction reference. The verification process is responsible for updating the equation by calculating the measurement, combining the estimated value of the last time state and the current measurement variable. This process is responsible for feeding back information and building an improved posterior estimate of the current state.

Time update equation

$$\hat{X}_{k^-} = A\hat{X}_{k-1} + B\hat{U}_{k-1}. \tag{6}$$

Inductive time update equation

$$P_{k^-} = AP_{k-1}A^T + Q. \tag{7}$$

State update equation

$$K_k = P_{k^-}H^T\left(HP_{k^-}H^T + R\right)^{-2}. \tag{8}$$

Inductive state update equation

$$\hat{X}_k = \hat{X}_{k^-} + K_k\left(Z_k - H\hat{X}_{k^-}\right). \tag{9}$$

The application of Kalman filter in path tracking is shown in Figure 5.

As shown in Figure 5, suppose the state vector of the target at time $k$ is expressed as follows:

$$X_k = \left[x_k, y_k, x_k{}', y_k{}'\right]^T. \tag{10}$$

The position of the target is selected as the observation vector and expressed as follows:

$$\mathrm{z(k)} = [\mathrm{xc_k}, \mathrm{yc_k}]^{\mathrm{T}}. \tag{11}$$

Assuming that the center of the target changes and accelerates linear motion, the acceleration changes randomly and obeys the Gaussian distribution, according to Newton's law of motion:

$$\begin{aligned} x_k &= x_{k-1} + x_{k-1}t + \tfrac{1}{2}w_{k-1}t^2, \\ y_k &= y_{k-1} + y_{k-1}t + \tfrac{1}{2}w_{k-1}t^2, \\ x_k' &= x_{k-1}' + w_{k-1}t^2, \\ y_k' &= y_{k-1}' + w_{k-1}t^2. \end{aligned} \tag{12}$$

Since there is no control quantity, $B = 0$ have to

$$\begin{bmatrix} xc_k \\ yc_k \end{bmatrix} = \begin{bmatrix} 1 & 0 & 0 & 0 \\ 0 & 1 & 0 & 0 \end{bmatrix} \begin{bmatrix} x_k \\ y_k \\ x_k' \\ y_k' \end{bmatrix} + \begin{bmatrix} 1 \\ 1 \end{bmatrix} v_k. \tag{13}$$

Thus, the state transition matrix is obtained as follows:

$$A_k = \begin{bmatrix} 1 & 0 & t & 0 \\ 0 & 1 & 0 & t \\ 0 & 0 & 1 & 0 \\ 0 & 0 & 0 & 1 \end{bmatrix}. \tag{14}$$

Thus, the state transition matrix is obtained as follows:

$$H_k = \begin{bmatrix} 1 & 0 & 0 & 0 \\ 0 & 1 & 0 & 0 \end{bmatrix}. \tag{15}$$

According to the above parameters, the prediction function of Kalman filter can be effectively realized.

(2) Single-target long-time algorithm

In this paper, the selected feature points are represented by yellow dots (see the overall architecture diagram of the algorithm for details), the feature points are tracked, and their positions in the current frame are found according to the optical flow method. Using the single-target long-term algorithm to track the feature points, the tracking is based on the optical flow method pathfinding mechanism, and traverse to find the position of the feature points in the current frame. In addition, a $10 \times 10$ matrix is established with each feature point as the center, and the similarity of the normalization coefficient of the feature point matrix of the $t$-th frame and the feature point matrix of the $t + 1$-th frame is calculated:

$$\mathrm{NCC} = \sum_{x,y} [f(x,y) - f_{u,v}][t(x-u, y-v) - t]. \tag{16}$$

Finally, the median of the offsets of all remaining feature points in the $x$-direction and $y$-direction is calculated as the offset value of the target in the current frame:

$$\mathrm{NCC}' = \left\{ \sum_{x,y} [f(x,y) - f_{u,v}]^2 \sum_{x,y} [t(x-u, y-v) - t]^2 \right\}^{0.5}. \tag{17}$$

The positive nearest neighbor similarity is defined as follows:

$$S^+(p, M) = \max_{p_i^+ \in M} S(p, p_i^+). \tag{18}$$

The negative nearest neighbor similarity is as follows:

$$S^-(p, M) = \max_{p_i^- \in M} S(p, p_i^-). \tag{19}$$

The relative similarity between the image element and the target model is as follows:

$$S^r = \frac{S^+}{S^+ + S^-}. \tag{20}$$

Single-target long-term algorithm takes one or more image elements output by the monitor as the monitoring result, combines the monitoring result with the integrated module tracker, and outputs the final tracking result.

## 3. Experiment Results of Path Tracking Algorithm

Path tracking algorithm improvement steps: First, an initial frame is added for the target to be tracked. Secondly, it analyzes the initial state information of the target to be tracked in the initial frame to complete the initialization of the Kalman filter and the single-target long-time algorithm. Then, the monitoring frame is expanded according to the boundary points of the target, and the scanning range of the monitor is enlarged, so as to facilitate the monitoring of the target within this range. Finally, if the target is located, the parameters such as the latitude and longitude of the target, the center point, and the boundary point are output. If the target position cannot be located, it loops traversal until the target is located.

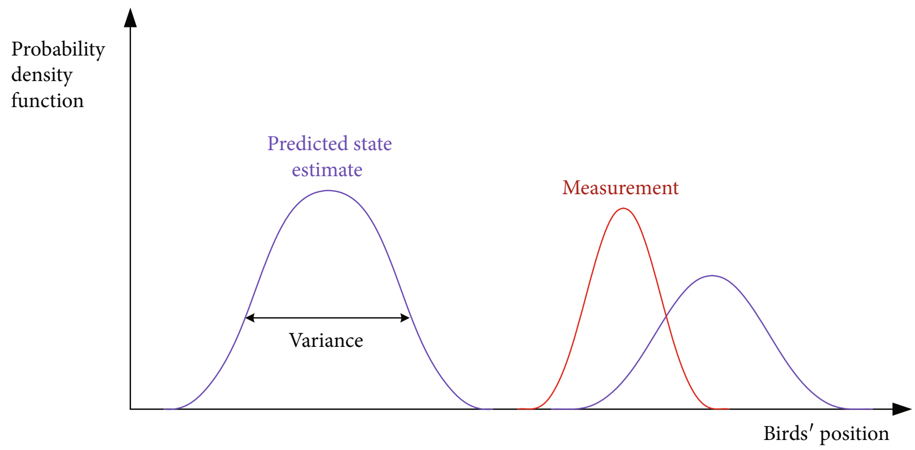


Figure 5: Kalman filter applied to path tracking.

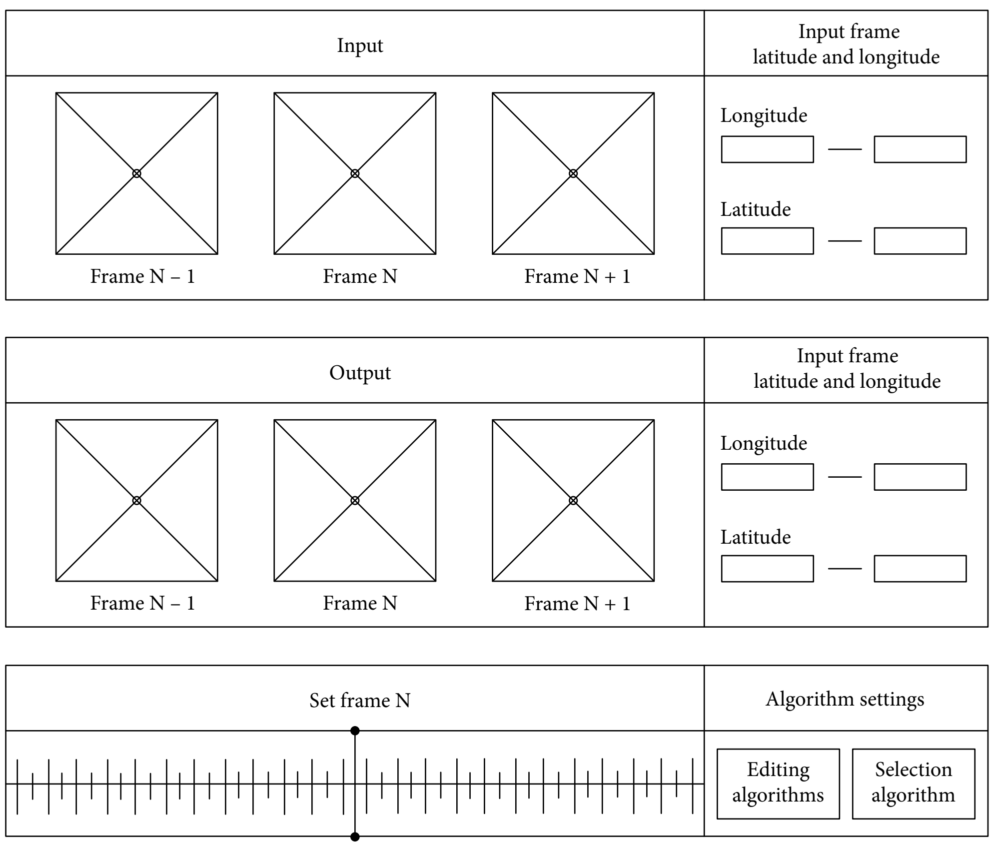


Figure 6: Test of system design.

In this paper, the improved algorithm is named IRSM-TLD, and the unimproved single-target long-time algorithm is named TLD. The proposed improved path tracking algorithm scheme has been described above, and the analysis of specific problems in two cases is given. Next, the feasibility of the improved algorithm proposed in this paper will be proved through experimental tests. The test system design is shown in Figure 6.

As shown in Figure 6, this paper designs a system based on image processing and used to monitor change information in the early stage of the experimental test.

(1) Set the sample set

This paper collects 100 groups of migratory bird flight videos in the network for testing samples, each group of

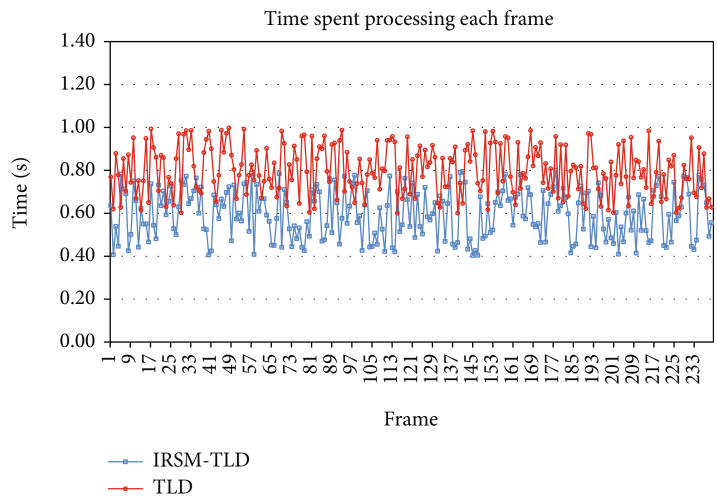


Figure 7: Time spent processing each frame.

videos consists of 240 frames, and the video size is uniformly adjusted to $1280 \times 720$ pixels. The video is composed of differentiated pictures, which are divided into simple background, strong light background, and complex background. In the early stage of the experiment, a large number of preprocessing tests were carried out on the target. It involves the image matching, geometric correction, and radiometric correction described above, and the test is operated by the system designed above. The video uses 24 frames per second to ensure that the pixels of each frame will not jump too much compared to the previous frame, which is conducive to the smooth progress of the experiment.

(2) Experimental test and data

This paper defines three algorithm evaluation indicators, which are the algorithm "time spent processing each frame," "position overlap," and "center offset error." Each indicator can reflect the performance of the algorithm in a certain aspect. Among them, the indicator "time spent processing each frame" can reflect the real-time performance of the algorithm. When actually tracking the migration paths of egrets, the real-time requirements of the algorithm are very high. The more time the algorithm spends processing each frame, the more it will drag down the overall tracking speed and thus affect the tracking accuracy. The index of "location overlap" can reflect the graph inclusiveness of the algorithm. In the previous article, the superpixel segmentation based on graph theory was introduced, which can segment the frame image and locate the target position and contour. It compares the target position generated by the algorithm before and after the improvement with the actual target position of the screen, respectively, and get the comparison of the degree of overlap. The higher the degree of overlap, the more accurate the algorithm is. "Center offset error" is an advanced index of "position overlap." This indicator makes further judgment on the basis of position comparison, that is, to obtain the center point connected with each boundary point of the target, so as to make further positioning. The target center points generated by the algorithm before and after the improvement are compared with the actual target center points of the screen, respectively, and the center offset error situation is obtained. The lower the center offset error, the more accurate the algorithm is.

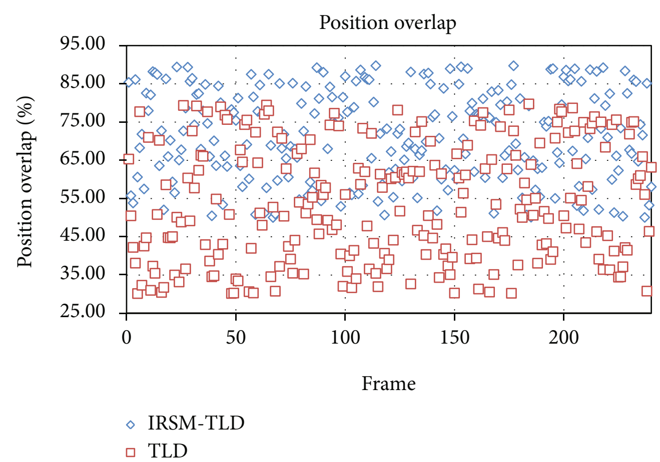


Figure 8: Position overlap.

After the experimental test of three indicators

(1) The comparison of the time taken by the unimproved algorithm and the improved IRSM-TLD algorithm to process each frame is shown in Figure 7.

From Figure 7, it can be concluded that the time interval used by the improved IRSM-TLD algorithm to process each frame is 0.4 s-0.8 s, and the time interval used by the unimproved TLD algorithm to process each frame is 0.6 s-1.0 s. It has significantly reduced processing time.

The comparison of the "position overlap" of the target measured by the unimproved algorithm and the improved IRSM-TLD algorithm is shown in Figure 8.

From Figure 8, it can be concluded that the location overlap range of the target measured by the improved IRSM-TLD algorithm is 50%-90%, and the location overlap

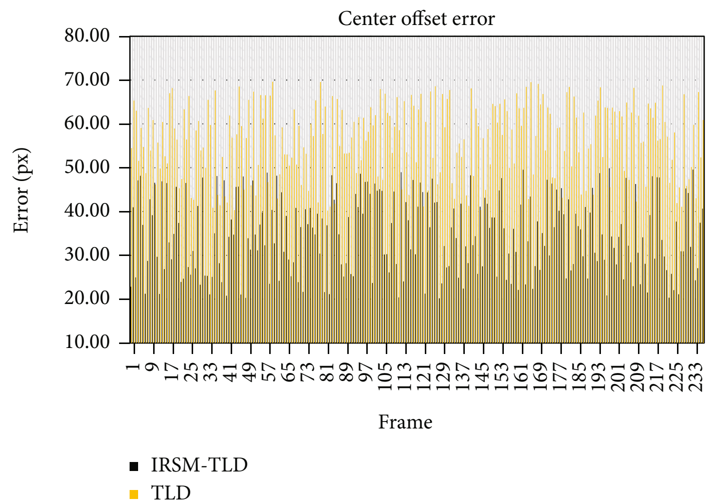


Figure 9: Center offset error.

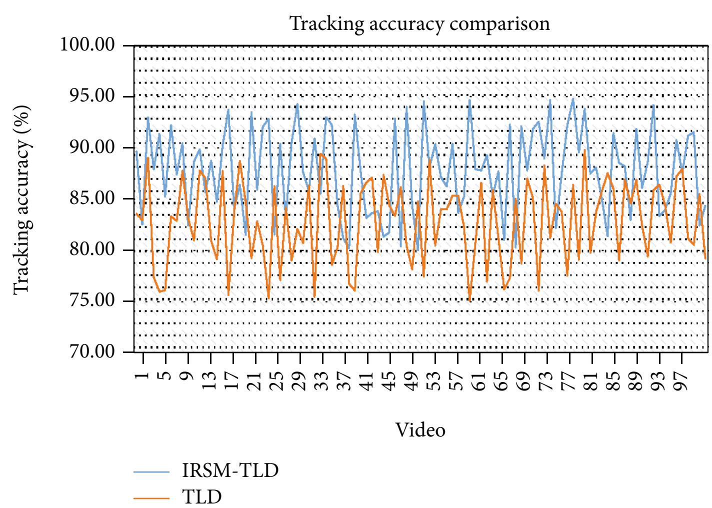


Figure 10: Tracking accuracy comparison.

range of the target measured by the unimproved TLD algorithm is 25%-80%. The position of the target measured by the improved IRSM-TLD algorithm is more accurate.

The comparison of the "center offset error" of the target measured by the unimproved algorithm and the improved IRSM-TLD algorithm is shown in Figure 9.

It can be concluded from Figure 9 that the center offset error of the target measured by the improved IRSM-TLD algorithm is generally lower than that of the unimproved TLD algorithm.

The three indicators are fused to calculate the tracking accuracy of the two algorithms on 100 video samples, as shown in Figure 10.

It can be seen from Figure 10 that the accuracy of the unimproved egret bird migration path tracking algorithm is between 70% and 90%, while the improved Egret bird migration path tracking algorithm based on intelligent remote sensing monitoring has an accuracy of 80% to 90% between 95%. After calculation, the improved algorithm improves the tracking accuracy by about 8.37% compared with the unimproved algorithm. The improved algorithm can better track the position of the egret bird target, so as to accurately obtain the migration path of the egret bird, and lay a solid foundation for the protection and research work of related scholars.

## 4. Conclusions

In this paper, the intelligent remote sensing monitoring technology is integrated into the research of the migratory path tracking algorithm of egrets, the method of removing image redundancy by artificial intelligence is used, and the tracking algorithm is improved by combining Kalman filter and single-target long-time algorithm. The improved algorithm is used to simulate 100 samples. From the test results, it can be concluded that the improved tracking algorithm in this paper can lock the location range of the target from the remote sensing image and track the target with high precision. Compared with the unimproved algorithm, it improves the tracking accuracy by about 8.37% and can obtain the migration path of the target more accurately, which is helpful for better protection and research of egrets, higher bird cognition level, and protection of the earth's ecology.

## Data Availability

No data were used to support this study.

## Conflicts of Interest

The author declares no conflicts of interest regarding the publication of this article.

## Acknowledgments

This work was supported by the Scientific Research Project of Hunan Provincial Department of Education (No.: 19c0654) and Science and Technology Development Plan of Hengyang City, Hunan Province (No.: 2010kj35).

## References

[1] Y. M. Dong, M. Li, Q. E. He et al., "Epigenome-wide tobacco-related methylation signature identification and their multi-level regulatory network inference for lung adenocarcinoma," *BioMed Research International*, vol. 2020, 12 pages, 2020.

[2] L. Yao, D. Hu, C. Zhao, Z. Yang, and Z. Zhang, "Wireless positioning and path tracking for a mobile platform in greenhouse," *International Journal of Agricultural and Biological Engineering*, vol. 14, no. 1, pp. 216–223, 2021.

[3] N. Zendehdel and M. Gholami, "Robust self-adjustable path-tracking control for autonomous underwater vehicle," *International Journal of Fuzzy Systems*, vol. 23, no. 2, pp. 6-7, 2020.

[4] O. Pannekoucke, R. Menard, and M. E. Aabaribaoune, "A methodology to obtain model-error covariances due to the discretization scheme from the parametric Kalman filter perspective," *Nonlinear Processes in Geophysics*, vol. 28, no. 1, pp. 1–22, 2021.

[5] C. A. Xia, X. Luo, B. X. Hu, M. Riva, and A. Guadagnini, "Data assimilation with multiple types of observation boreholes via the ensemble Kalman filter embedded within stochastic moment equations," *Hydrology and Earth System Sciences*, vol. 25, no. 4, pp. 1689–1709, 2021.

[6] E. Dong, M. Deng, J. Tong, C. Jia, and S. du, "Moving vehicle tracking based on improved tracking–learning–detection algorithm," *IET Computer Vision*, vol. 13, no. 8, pp. 730–741, 2019.

[7] P. Panda and M. Barczyk, "Blending of learning-based tracking and object detection for monocular camera-based target following - ScienceDirect," *IFAC-PapersOnLine*, vol. 54, no. 9, pp. 743–748, 2021.

[8] P. Quesada-Barriuso, D. B. Heras, and F. Argüello, "GPU accelerated waterpixel algorithm for superpixel segmentation of hyperspectral images," *The Journal of Supercomputing*, vol. 77, no. 9, pp. 10040–10052, 2021.

[9] Y. Chen, Y. Li, and J. Wang, "Remote aircraft target recognition method based on superpixel segmentation and image reconstruction," *Mathematical Problems in Engineering*, vol. 2020, 9 pages, 2020.

[10] P. Ding, Y. Zhang, P. Jia, and X. L. Chang, "A comparison: different DCNN models for intelligent object detection in remote sensing images," *Neural Processing Letters*, vol. 49, no. 3, pp. 1369–1379, 2019.

[11] M. Guo and S. Wang, "Remote sensing monitoring and ecological risk assessment of landscape patterning in the agro-pastoral ecotone," *Complexity*, vol. 2021, 13 pages, 2021.

[12] S. Riad, "Quantity of spring migration of migratory soaring birds over the Eastern Desert of Egypt," *Egyptian Academic Journal of Biological Sciences B Zoology*, vol. 12, no. 2, pp. 161–171, 2020.

[13] M. R. Braga, L. R. Jorge, and A. E. Jahn, "Future climate change will impact the migration of New World migrant flycatchers (Tyrannidae)," *Ornithology Research*, vol. 30, no. 1, pp. 63–74, 2022.

[14] P. Busse, "Estimation of local heading patterns of nocturnal migrants using orientation cages," *The Ring*, vol. 40, no. 1, pp. 31–58, 2018.

[15] L. Fragoso and J. Mora, "Overstory-understory land cover mapping at the watershed scale: accuracy enhancement by multitemporal remote sensing analysis and LiDAR," *Environmental Science and Pollution Research*, vol. 27, no. 1, pp. 75–88, 2020.

[16] K. Gromann, N. Roskamm, M. Budnik et al., "Konflikte als Hoffnungstrger. Auseinandersetzungen um die postmigrantische Stadtgesellschaft," *Neue Politische Literatur*, vol. 66, no. 3, pp. 305–322, 2021.

[17] H. Lu, Q. Liu, X. Liu, and Y. Zhang, "A survey of semantic construction and application of satellite remote sensing images and data," *Journal of Organizational and End User Computing (JOEUC)*, vol. 33, no. 6, pp. 1–20, 2021.

[18] Z. Xing and G. Li, "Intelligent classification method of remote sensing image based on big data in spark environment," *International Journal of Wireless Information Networks*, vol. 26, no. 3, pp. 183–192, 2019.

[19] D. Yin, R. Hou, and J. Du, "SAR image change detection method based on intuitionistic fuzzy C-means clustering algorithm," *Journal of Intelligent and Fuzzy Systems*, vol. 38, no. 4, pp. 3595–3604, 2020.

[20] X. Wang, J. Liu, O. I. Khalaf, and Z. Liu, "Remote sensing monitoring method based on BDS-based maritime joint positioning model," *CMES-Computer Modeling in Engineering & Sciences*, vol. 127, no. 2, pp. 801–818, 2021.

[21] S. Shen, P. Yue, and C. Fan, "Quantitative assessment of land use dynamic variation using remote sensing data and landscape pattern in the Yangtze River Delta, China," *Sustainable Computing-Informatics & Systems*, vol. 23, pp. 111–119, 2019.

[22] M. K. Yuan, L. Q. Dai, D. M. Yan, L. Q. Zhang, J. Xiao, and X. P. Zhang, "Fast and error-bounded space-variant bilateral filtering," *Journal of Computer Science and Technology*, vol. 34, no. 3, pp. 550–568, 2019.

[23] S. Pang, X. Hu, M. Zhang, Z. Cai, and F. Liu, "Co-segmentation and superpixel-based graph cuts for building change detection from bi-temporal digital surface models and aerial images," *Remote Sensing*, vol. 11, no. 6, pp. 729–729, 2019.